AGU PUBLICATIONS

JGR

Journal of Geophysical Research: Space Physics

RESEARCH ARTICLE
10.1002/2016JA022657

Key Points:
- Comparison between THEMIS satellite data and ground-based optical auroral data proves that cusp auroras are on open field lines
- The source of the dayside cusp auroral particles is the magnetosheath
- The soft cusp auroras contain significant N_2^+ intensity to imply that acceleration of the magnetosheath particles takes place

Supporting Information:
- Supporting Information S1
- Data Set S1
- Data Set S2
- Data Set S3
- Data Set S4
- Data Set S5
- Data Set S6
- Data Set S7
- Data Set S8
- Data Set S9
- Data Set S10

Correspondence to:
S. B. Mende,
mende@ssl.berkeley.edu

Citation:
Mende, S. B., H. U. Frey, and V. Angelopoulos (2016), Source of the dayside cusp aurora, *J. Geophys. Res. Space Physics*, *121*, 7728–7738, doi:10.1002/2016JA022657.

Received 3 MAR 2016
Accepted 17 JUL 2016
Accepted article online 19 JUL 2016
Published online 22 AUG 2016

Source of the dayside cusp aurora

S. B. Mende[1], H. U. Frey[1], and V. Angelopoulos[2]

[1]Space Sciences Laboratory, University of California, Berkeley, California, USA, [2]IGPP, ESS, University of California, Los Angeles, California, USA

Abstract Monochromatic all-sky imagers at South Pole and other Antarctic stations of the Automatic Geophysical Observatory chain recorded the aurora in the region where the Time History of Events and Macroscale Interactions during Substorms (THEMIS) satellites crossed the dayside magnetopause. In several cases the magnetic field lines threading the satellites when mapped to the atmosphere were inside the imagers' field of view. From the THEMIS magnetic field and the plasma density measurements, we were able to locate the position of the magnetopause crossings and map it to the ionosphere using the Tsyganenko-96 field model. Field line mapping is reasonably accurate on the dayside subsolar region where the field is strong, almost dipolar even though compressed. From these coordinated observations, we were able to prove that the dayside cusp aurora of high 630 nm brightness is on open field lines, and it is therefore direct precipitation from the magnetosheath. The cusp aurora contained significant highly structured N_2^+ 427.8 nm emission. The THEMIS measurements of the magnetosheath particle energy and density taken just outside the magnetopause compared to the intensity of the structured N_2^+ 427.8 nm emissions showed that the precipitating magnetosheath particles had to be accelerated. The most likely electron acceleration mechanism is by dispersive Alfvén waves propagating along the field line. Wave-accelerated suprathermal electrons were seen by FAST and DMSP. The 427.8 nm wavelength channel also shows the presence of a lower latitude hard-electron precipitation zone originating inside the magnetosphere.

1. Introduction

It has been recognized for a long time that the dayside cusp aurora is produced by soft particle precipitation [*Heikkila and Winningham*, 1971; *Winningham and Heikkila*, 1974]. Solar wind interaction with Earth's magnetic field produces the dayside cusps, and it was suggested that here the solar wind might have direct access to the magnetosphere. The electron precipitation near the cusp region is characterized by low energies, less than 500 eV [e.g., *Heikkila and Winningham*, 1971; *Winningham and Heikkila*, 1974; *Shepherd et al*., 1976; *Newell et al*., 2006]. Low-energy electrons produce auroras that are emitted at high altitudes, producing relatively intense emissions of the long lifetime oxygen emission at 630 nm. The auroras in the cusp were found to emit very intense 630 nm emission [*Eather and Mende*, 1971]. *Johnsen et al*. [2012] argue that the altitude of the 630 nm emission in the cusp aurora is highly variable, and *Lockwood et al*. [1993] determined the altitude of 630 nm emission peaks by comparing the latitudinal velocity of the 630 nm aurora with the velocity of emissions originating at lower altitude. There is no doubt that the emission height strongly depends on the mean energy of the precipitating electrons. The source of the electrons, and whether they undergo acceleration as they descend along the field line from the magnetosheath, are central issues in magnetosphere-ionosphere coupling.

When the interplanetary magnetic field (IMF) B_z is negative, the last closed field line maps to the dayside magnetopause in the subsolar region. We can define the surface of the last closed field lines on the dayside as the open/closed field line boundary or OCB. When B_z is negative, the OCB and the dayside reconnection X line are located at the subsolar magnetopause. The cusp aurora maps into the dayside magnetosphere, and the exact location of where it maps to, compared to the OCB, is important information. For example, the plasma flow across the OCB can be interpreted as the magnetopause reconnection rate [*Lockwood et al*., 2005]. The latitudinal location of the OCB is the dayside boundary of the total amount of open magnetic flux in the magnetosphere [e.g., *Hubert et al*., 2006; *Milan et al*., 2007], and it is an important parameter in maintaining the balance of magnetic reconnection at the magnetopause on the dayside and in the magnetotail on the nightside.

There have been many attempts at determining the location of the dayside cusp, which is the ionospheric foot point of the OCB. HF radars provide a signature through the spectral width of the backscattered signal,

which is characteristic of cusp precipitation [*Chisham et al*., 2005]. From low-altitude satellites carrying particle detectors [e.g., *Newell et al*., 2009, and references therein], one may look for the equatorward edge of soft magnetosheath-like precipitation of electrons and the characteristic signature of ion energy dispersion (velocity filter effect), and a transition to harder precipitation from the dayside extension of the central plasma sheet, which is maintained by trapped particles drifting from the dayside [*Eather et al*., 1979]. From satellites, the OCB has been inferred from the poleward boundary of the far-ultraviolet auroral oval [*Hubert et al*., 2006; *Longden et al*., 2010]. From the ground, the optical signature of these particle detector signatures (at least for electron precipitation) is easily recognizable by the existence of a red-dominated cusp aurora with a high red/blue ratio [*Eather and Mende*, 1971; *Eather et al*., 1979] or a high red/green ratio [*Sandholt et al*., 2002]. The OCB should be located somewhere near the optically detected cusp aurora.

In 2007/2008 the Time History of Events and Macroscale Interactions during Substorms (THEMIS) satellites [*Angelopoulos et al*., 2008] provided unprecedented opportunities for monitoring the dayside magnetospheric boundary and the relationship between the OCB and the cusp auroras that were observed by the monochromatic imagers at South Pole and other Antarctic stations of the Automatic Geophysical Observatories (AGO) chain [*Rosenberg*, 2000; *Mende et al*., 2009]. At every crossing, the THEMIS satellites provided an accurate location of the magnetopause, which is the same as the OCB. In addition, the THEMIS satellites measured the IMF near the magnetopause, eliminating the uncertainties associated with distant measurements of the IMF from satellites like Wind and ACE. The THEMIS satellites also provided measurements of the magnetosheath plasma density and mean particle energy, allowing the comparison of those parameters to the observed cusp auroras.

In this study, we will focus on investigating dayside magnetospheric boundaries. It is widely believed that magnetic field models, e.g., the Tsyganenko-96 field model [*Tsyganenko*, 1995], should accurately map the position of the magnetopause boundaries on the dayside, where the field lines are relatively short and not as distorted as on the nightside. Therefore, the determination of the position of the foot point of the magnetospheric boundaries at the time the satellites cross the magnetopause provides a clear measure of the location of foot point of the last closed field line. This provides a clear way to identify the location of the various types of dayside cusp auroras relative to the open/closed field line boundary.

We mapped each THEMIS satellite positions with the Tsyganenko-96 field model in 10 min steps using the instantaneous *Dst* value; the propagated solar wind dynamic pressure; and the IMF *x*, *y*, and *z* components. The traced field line data for each THEMIS satellite are appended to this paper as supporting information. The files show the date and time of mapping, the true spacecraft position in GSE coordinates (in Earth radii), the GSM positions of the first closed field line along the radius vector (in Earth radii), the *Dst* value that was used for the model, the solar wind dynamic pressure, the IMF, and the mapped foot point positions in geographic coordinates.

The stepwise increase in the magnetic field and the simultaneous drop in the plasma density measured by the THEMIS satellites provide a clear indication of a magnetopause crossing. However, almost always we see not just one but multiple magnetopause crossings caused by the rapid in-and-out motion of magnetopause. The simultaneous THEMIS data monitoring of the solar wind pressure and the IMF field show that a large fraction of these movements appear to be spontaneous and were not related to external impulses from the solar wind plasma or the variability of the IMF. At times, however, these motions can be identified as responses to pressure pulses or changes in the IMF.

It should be noted that the opportunities were relatively few when the THEMIS satellites were in the field of view of the Antarctic all-sky imager, near magnetic midday, and while crossing the magnetopause. In this study, we will conduct two case studies, 12 August 2007 and 23 July 2008, when these conditions were met.

2. Case Study: 12 August 2007

On 12 August 2007, the THEMIS satellites entered the magnetosphere when the magnetic foot points of each satellite were in the South Pole all-sky camera's field of view. During this initial part of the THEMIS mission, the satellites were moving essentially on the same orbit trajectory in a string-of-pearl configuration, with THEMIS B leading the pack. At the beginning of this period, the satellite foot points projected on the auroral ionosphere are shown at the bottom right of Figure 1 at 12:00 UT. Note that when a satellite was outside the magnetopause, it was not possible to map the field line of the satellite down to the atmosphere. To

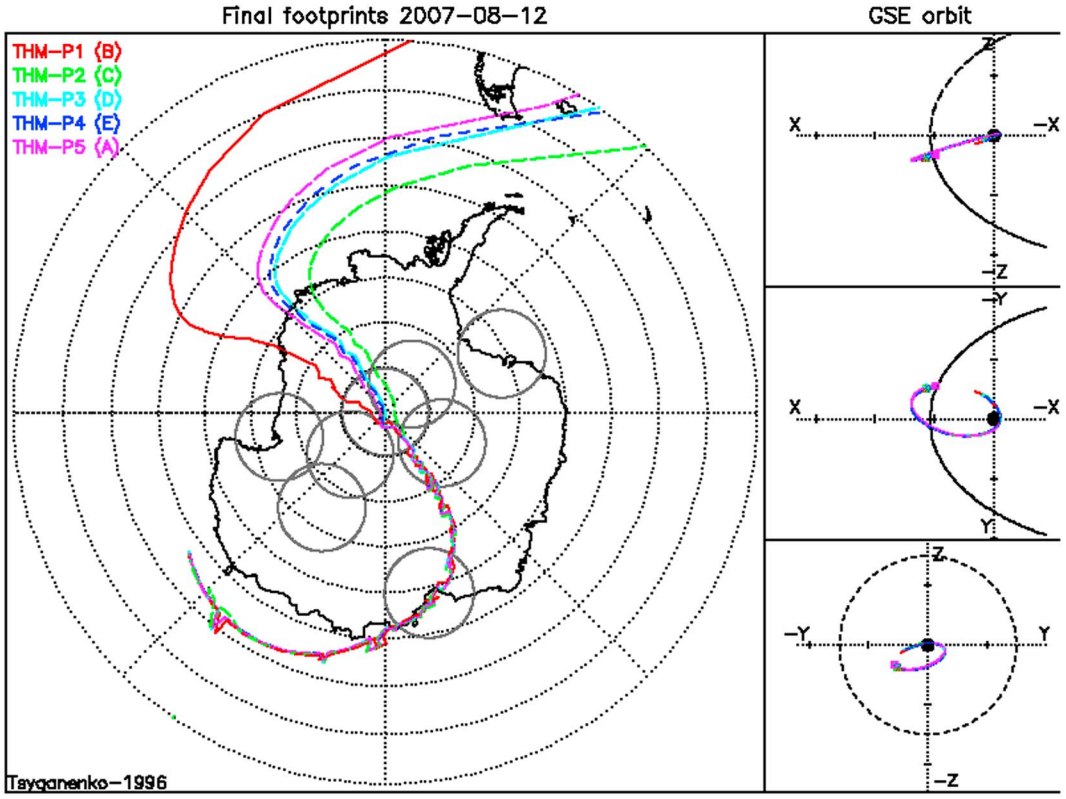

Figure 1. THEMIS satellite foot points as projected on the Earth atmosphere for the 12 August 2007 conjunction. When the satellites are outside the magnetosphere before 14:30 UT, the plots show the magnetic foot point of the first closed field line at the intersection of the satellite's radius vector and the magnetopause, and the foot points of the various satellites appear to coincide. When the satellites are inside the magnetosphere, their foot points are individually projected along the local magnetic field line as described by the Tsyganenko 1996 model.

represent the position of the satellites on the map projections, we instead chose to map the field line passing through the intersection of the magnetopause and the radius vector of the satellite. The satellites followed one another in the order THM B, C, D, E, and A, and their mapped radius vector trajectories seemed to approximately coincide while they were outside the magnetosphere, but when they entered the magnetosphere, then the projection of the tracks seemed to separate due to the resolvable difference among their positions. The first satellite to enter the magnetosphere is THM B, illustrated in red, and it is shown to peel off first from the common trajectory. It is followed by C, then D, E, and finally, A.

Figure 2 (first and second panels) show the keograms from ground stations P1 (Figure 1) and South Pole (SP). The summary plots for THM B, the lead satellite (Figure 2, third and fourth panels), and THM A, the last of the satellites (Figure 2, fifth and sixth panels). Ground station P1 is on the same magnetic meridian as the South Pole, where P1 is at about $-80°$ magnetic latitude while South Pole is at $-74.5°$. This was a fairly quiet day, and the dayside cusp aurora was on the poleward horizon at South Pole (SP) and on the equatorward horizon at A1. The two stations are viewing the same aurora, except from a different perspective.

In Figure 2, third to sixth panels, we show the three-component magnetic measurements [*Auster et al.*, 2008] and the plasma density for the leading (THM B) and for the tail end (THM A) satellites. For the magnetometer, the B_z component is illustrated in red. The magnetometer shows an upward jump to >20 nT when the satellite crosses the magnetopause boundary and enters the magnetosphere. At the same time, the sheath density of $>10\,\mathrm{cm}^{-3}$ drops to less than $1\,\mathrm{cm}^{-3}$. It is quite clear from the satellite data that THM B first encounters the magnetopause around 14:00 and is firmly inside the magnetosphere by 14:40. THM A first encounters the magnetosphere around 14:30 but takes several hours until 17:00 before it is beyond the magnetopause fluctuations and firmly inside the magnetosphere. We have drawn three vertical lines to highlight latitudinal excursion events in the keograms. The first one is an equatorward motion at 15:20. It looks that

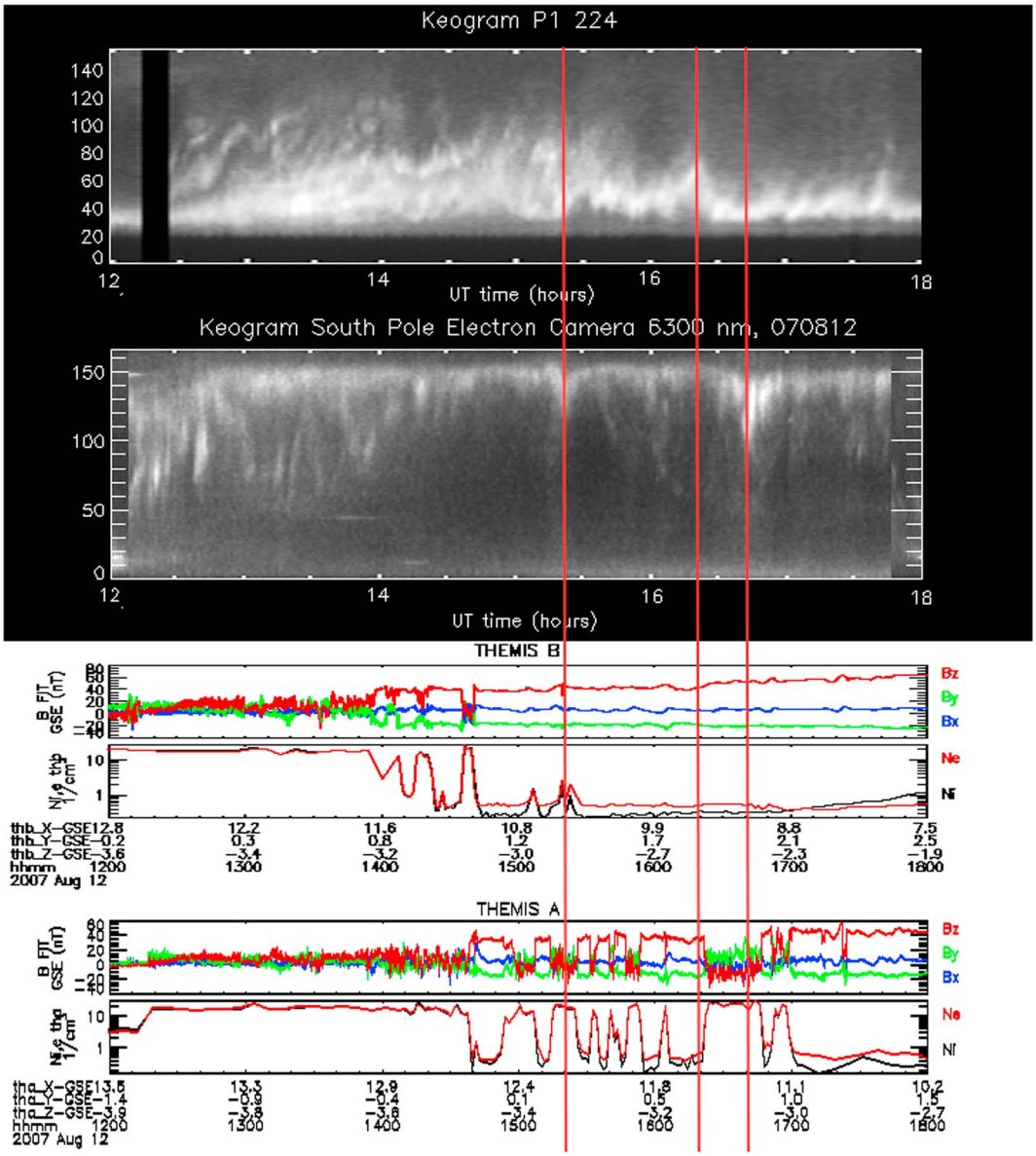

Figure 2. Keogram plots of 630 nm emission for (first panel) P1 and for (second panel) South Pole, (third and fourth panels) THEMIS B magnetometer data and plasma density data, and (fifth and sixth panels) the same for THEMIS A. THEMIS satellites were in a string-of-pearl configuration with THM B leading and THM A trailing last.

THM B, which was already in the magnetosphere, got some plasma density enhancement from this inward motion of the magnetopause, which is consistent with its being back into the magnetosheath and with an equatorward movement of the cusp auroral region. The second red line pair is shown denoting an equatorward excursion of the dayside aurora from a maximum poleward position at 16:20 to a minimum at 16:40. THM B is far inside the magnetosphere at this time, and there is no response. THM A was also inside the magnetosphere at the start of this period, as seen from the magnetic field B_z magnitude and plasma density. One can argue that the equatorward motion of the aurora boundary put THM A temporarily back in the magnetosheath to see increased magnetosheath plasma density and low magnetic field. After 16:40, THM A is soon back into the magnetosphere.

From the above, we can observe that THM B entered the magnetosphere at around 14:45 and THM A at 17:00 UT, and after that, all the satellites were on closed field lines.

In Figure 3, we mapped the aurora onto a geographic latitude-longitude grid. The red 630 nm emission (Figure 3, left) was displayed with an assumed emission altitude of 200 km while the 427.8 nm (Figure 3, right)

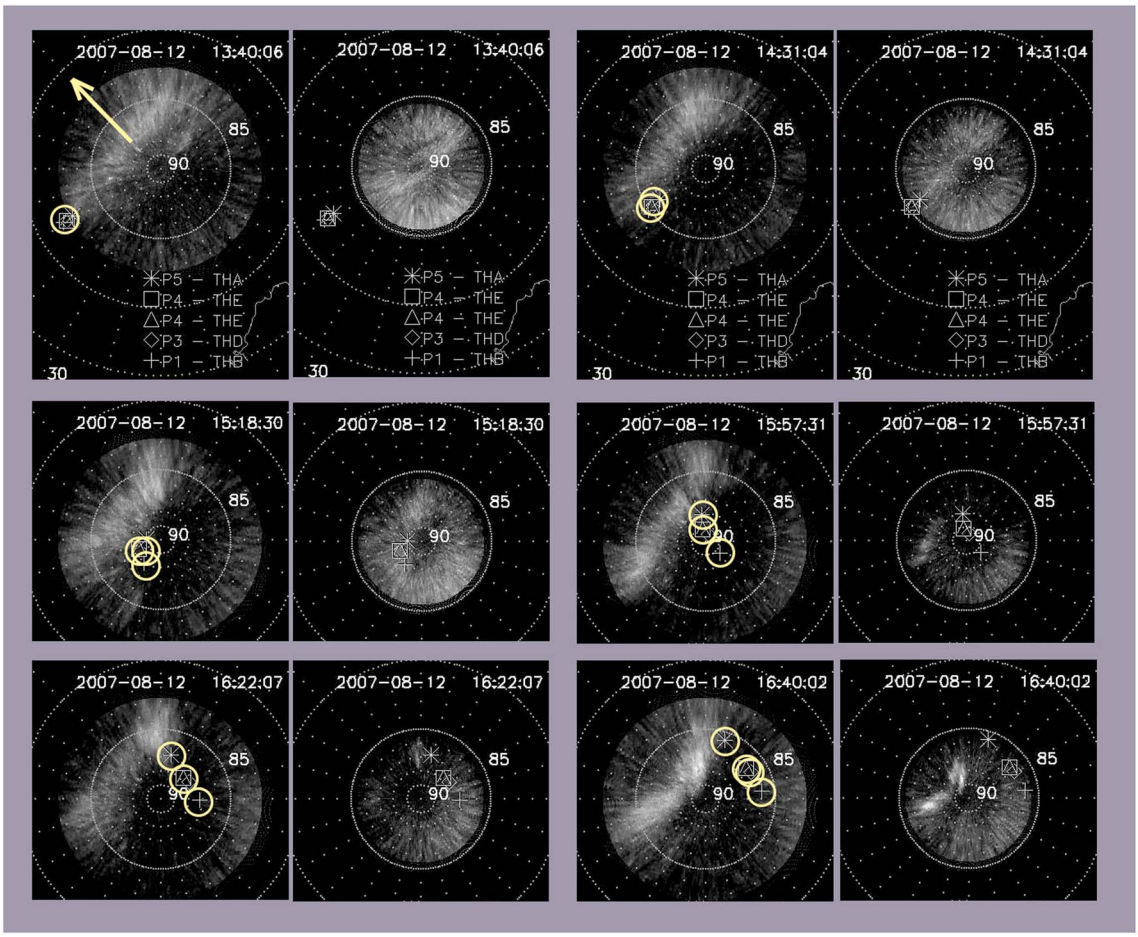

Figure 3. Collage of ground-projected all-sky images of the dayside (left) 630 nm aurora and (right) 427.8 nm taken by the South Pole all-sky imager. The foot points of the THEMIS satellites are mapped to the aurora. The direction toward the magnetic pole is shown in the 13:40:06 frame by an arrow pointing up and to the left. Magnetic midday is at 15:30 UT at South Pole.

with 110 km. In the first few frames, at 13:40:06 and at 14:31:04, the coincidence of the mapped foot points of all the satellites indicates that they had a common radius vector and were all outside of the magnetosphere. At 14:31:04, THM B (shown as cross) starts separating from the others, and by 15:18:30 it is completely separate, showing that THM B had entered the magnetosphere and its latitude position should mark the magnetopause and the last closed field line. Satellites THEMIS C, D, E, and A slowly move apart between 15:18:30 as the satellites gradually enter the magnetosphere. The last satellite to enter is THM A, which enters the magnetosphere at about 16:40.

The most significant conclusion is that when they enter the magnetosphere, the foot points of the satellites are all on the equatorward side of the 630 nm aurora. Thus, the midday aurora, primarily seen in 630 nm emission, is on the poleward side of the mapped positions of the satellites when they enter the magnetosphere, and therefore, they are on open field lines.

In the collage of Figure 3, we have also included the simultaneously taken 427.8 nm images. To produce 427.8 nm emission of any significant intensity, it is necessary to have precipitating electrons in the energy range of several tens of eVs.

The fairly persistent equatorward precipitation is seen on most frames but only in the 427.8 nm emission. This emission is located equatorward of the latitude of the mapped magnetopause crossings and therefore inside the magnetosphere. It is most likely to be precipitation from energetic ring current electrons (or protons) that drifted around from the nightside on closed field lines [*Eather et al.*, 1979; *Sandholt et al.*, 2002].

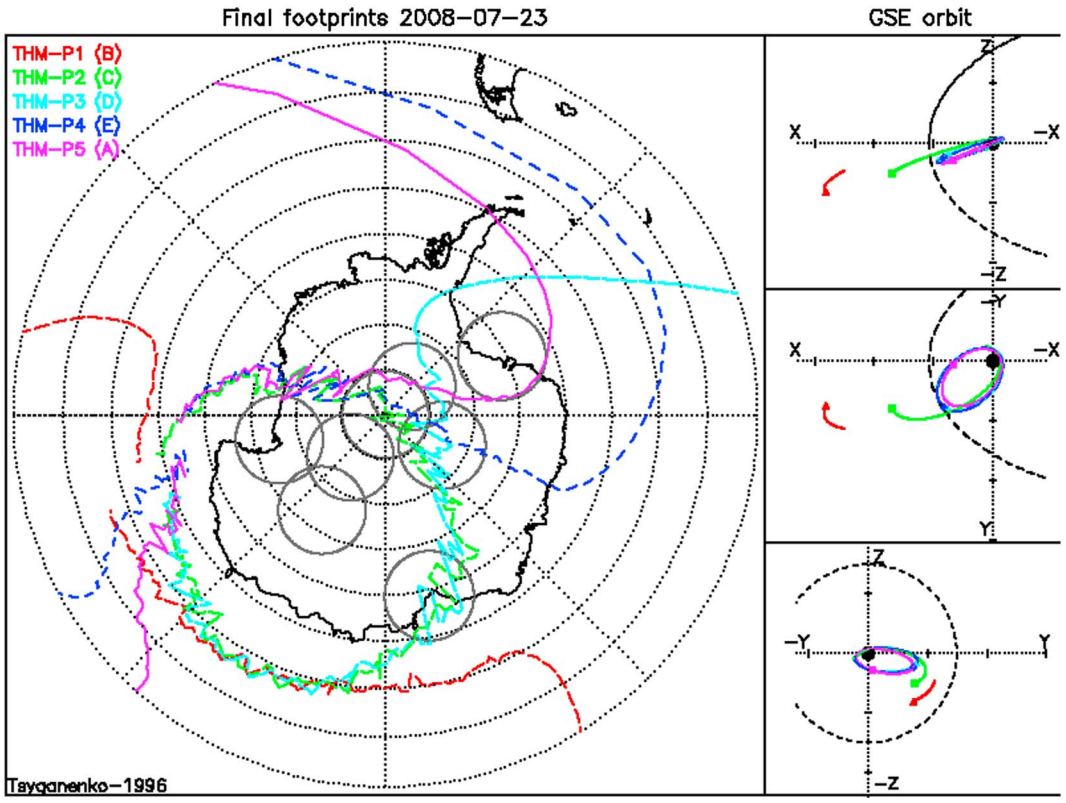

Figure 4. THEMIS satellite foot points and orbit trajectories for 23 July 2008. THM B is not shown on the auroral foot point trajectories because it was clearly outside and in front of the magnetosphere during the whole day. THM C, THM D, THM E, and THM A are shown when inside the magnetosphere with their foot point projected along the field line, as expressed by the Tsyganenko 1996 model. When these satellites are outside of the magnetosphere, the plots show the magnetic footprint of the intersection of the satellite's radius vector and the magnetopause.

As we have seen, the poleward region of the soft precipitation observed in high-intensity 630 nm emission is outside the magnetosphere on open field lines and the source of the electrons has to be the magnetosheath. The THEMIS measurements of the magnetosheath particle energy and density can be compared to the intensity of the optical aurora to determine whether there are any acceleration processes occurring on the cusp field lines.

3. Case Study 2: 23 July 2008

In 2008, the THEMIS satellites were injected into their intended orbit configuration, and with the exception of THM D and E, they were placed on substantially different orbits. A good opportunity for coordinated observations of the dayside aurora at South Pole and at P1 of the AGO network and the THEMIS spacecraft occurred on 23 July 2008. Figure 4 (left) shows the THEMIS magnetic foot points, and on the right are two projections of the 3-D orbits of the THEMIS satellites. From the orbit projections on the right, we can see that THM B (P1) shown in red is about 25–27 R_E in front of the magnetosphere during the whole day. We use THM B as our solar wind plasma and IMF monitor.

In Figure 5 (first panel), we show the South Pole 630 nm keogram data. Figure 5 (second panel) shows the intensity of the aurora at South Pole, where the intensity values were taken at the foot points of the THM B, THM D, and THM E satellites. Figure 5 (third panel) is the ACE plasma pressure data showing that the solar wind provided a constant pressure. Figure 5 (fourth to sixth panels) are the THEMIS magnetometer data for THM B, D, and E. Since THM B is outside the magnetosphere, it measures the IMF field that drives reconnection and magnetospheric convection. It can be seen from this panel that the IMF field is highly variable during this period.

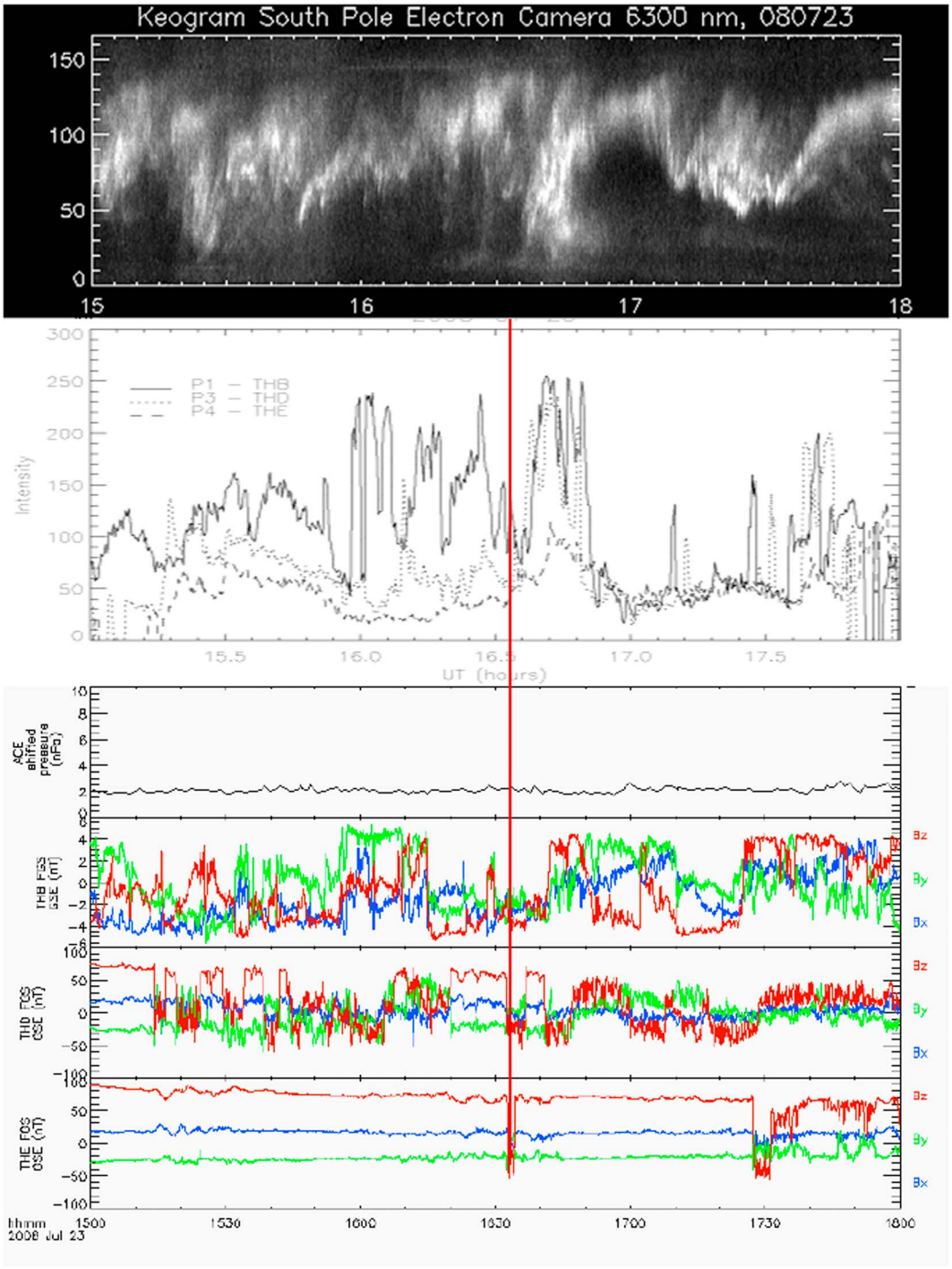

Figure 5. South Pole keogram (630 nm); South Pole auroral intensity at the footprint of THEMIS B, D, and E; ACE solar wind pressure; and THEMIS B, D, and E magnetometer data. THEMIS B is well outside and in front of the magnetosphere measuring the IMF in the solar wind. THEMIS D shows the positive B_z until about 15:15, when it crosses the magnetopause for the first time and is in the magnetosheath thereafter. THEMIS E is inside the magnetosphere until about 17:25 UT (relatively steady strong northward B_z).

At the beginning of the period, THM D magnetic field data (Figure 5, fifth panel) shows a B_z field of 70 nT, a typical field inside the magnetosphere, and it crosses the magnetopause first at about 15:15. After that, there is a long period with several magnetopause crossings until about 16:40. Subsequently, THM D shows much less B_z, consistent with the satellite being outside of the magnetopause. As we have discussed earlier, the

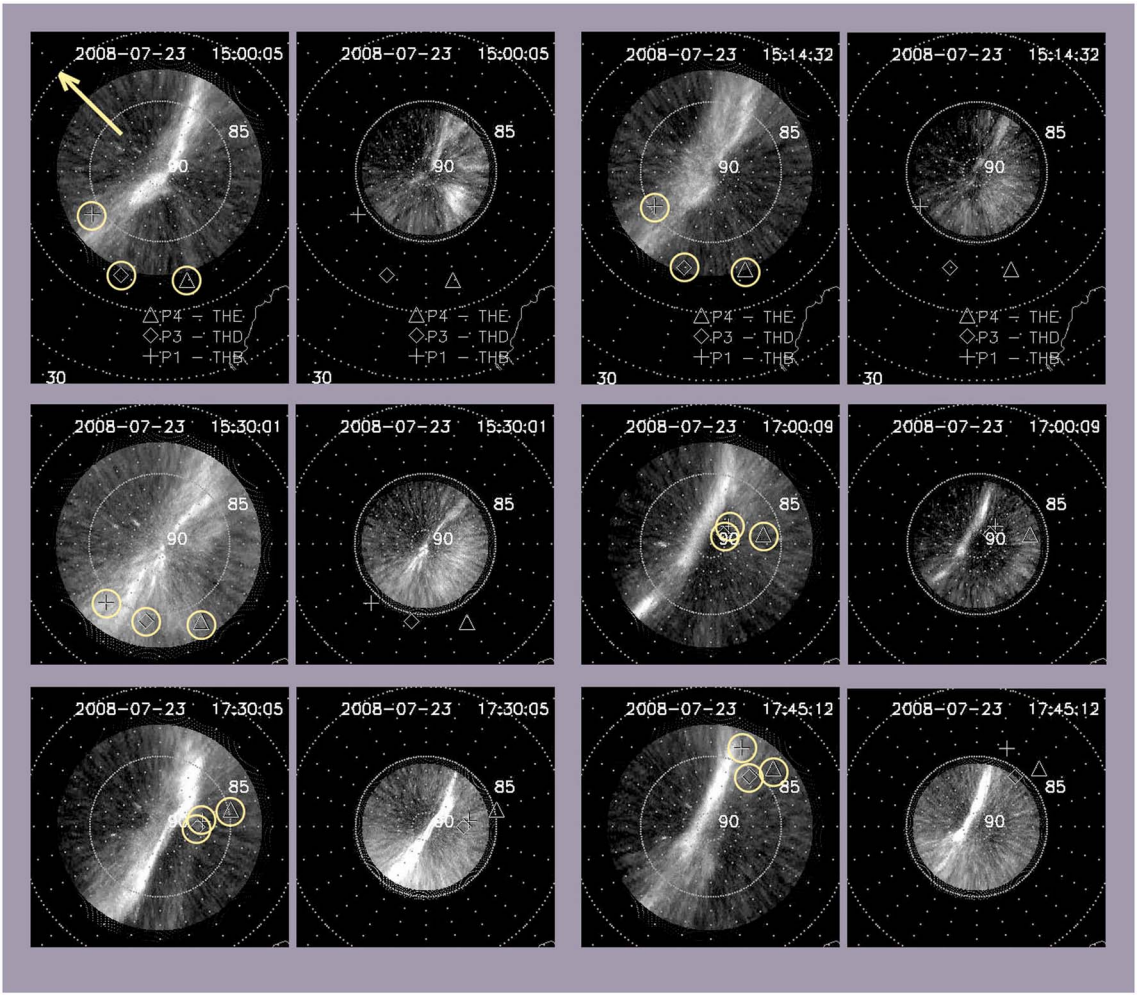

Figure 6. THEMIS satellite foot points mapped on the auroral ionosphere for 23 July 2008. The foot points of the THEMIS satellites are illustrated on each auroral image. The direction toward the magnetic pole is shown by an arrow pointing upward and toward the left.

magnetopause rapidly moved radially in and out, causing repeated magnetopause crossings. The in-and-out motions could be caused by surface waves, but since the solar wind pressure was almost constant and IMF B_z was negative, the more likely cause was multiple flux transfer events. On the other hand, some of the magnetopause motion can be attributed to IMF field driving. For example, there is an extended period of negative B_z from 16:12 to 16:42, as shown by THM B. We see a B_z negative response at THM D lasting from about 16:33 to about 16:38. Interestingly, there is a response even at THM E between about 16:33 and 16:36. Did the magnetopause get pushed in as far as THM E? There is some evidence in the keogram that the oval was pushed significantly equatorward at this point in time.

In Figure 6, we represent the magnetic foot points of the THEMIS satellites superimposed on the 630 nm OI and the 427.8 nm emission auroral images, using the same Tsyganenko field model that was used to produce Figure 3. We followed the same procedure as before, and when a spacecraft was inside the magnetosphere, the magnetic foot point is mapped using the *Tsyganenko* [1995] field model. When the satellite was outside the magnetosphere, we map the intersection of the satellite's radius vector and the magnetopause.

At 15:00:05, only the THM B apparent foot point is in the South Pole camera's field of view (FOV) and THM D and THM E are just outside the FOV of the 630 nm camera. THM B is out of the magnetosphere, but its foot point, which is in the magnetopause location, maps on top of the 630 nm aurora. This alone indicates that the field lines connecting the aurora are also outside the magnetopause. We noted from Figure 5 that THEMIS D crosses the magnetopause at about 15:15 and THEMIS E at about 17:25 UT. We can determine the position of

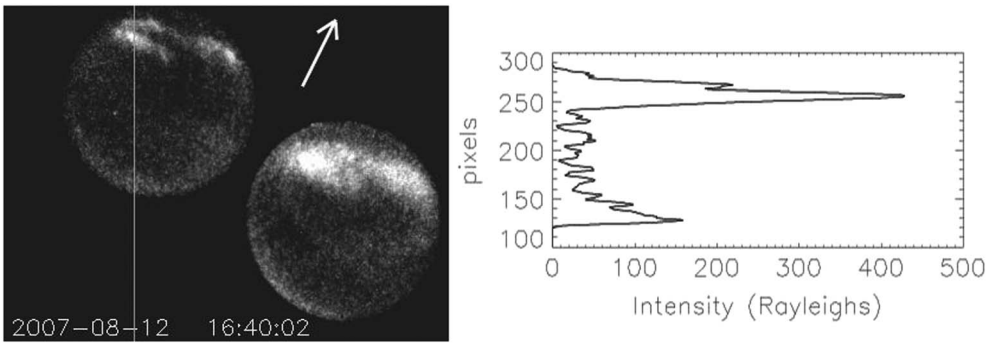

Figure 7. The 427.8 nm intensity profile. (left) Original image in the 427.8 nm all-sky field with marker line showing where the profile is taken. (right) Intensity profile along that line is shown.

these footprints with respect to the aurora on the collage of Figure 6. The magnetopause footprint is represented by an imaginary line between the footprint of the satellite THM D at 15:14:32 (shown as a diamond shape) and the footprint of THM E at 17:30:05 (shown as a triangle). This line is well equatorward of the more intense cusp precipitation shown on the 630 and 427.8 nm frames.

It should be noted that here we attributed the precipitation largely to soft electrons; however, significant ion precipitation is also expected [e.g., *Fuselier et al*., 2002].

4. Discussion

In the first case study, THEMIS satellites were on a string-of-pearl configuration on an elliptical orbit of about 14 R_E apogee. They made measurements in the solar wind and in the magnetosheath prior to crossing the magnetopause into the magnetosphere. Prior to entering the magnetosphere on 12 August 2007, and while inside the magnetosheath, THEMIS satellites measured a particle density of about 20 particles/cm^3 (see Figure 2, fourth and sixth panels) with energy of about 80 eV. The energy flux carried by such electrons is 1.27×10^{11} eV cm^{-2} or ~0.2 erg cm^{-2} s^{-1}. The efficiency of the auroral 427.8 nm emission production has been modeled by several groups [*Rees and Luckey*, 1974; *Strickland et al*., 1989; *Gattinger et al*., 1991]. Figure 6 of *Strickland et al*. [1989] shows that the 427.8 nm auroral intensity production is about 100 Rayleigh/(ergs cm^{-2} s^{-1}) for 100 eV electrons when the atmospheric O/N_2 ratio is in a normal range representing a quiescent atmosphere. Thus, the production efficiency of N_2^+ 427.8 nm with magnetosheath energy electrons with density of 20 cm^{-3} would produce about 130 Rayleigh (R) if they were to precipitate as aurora.

Although no absolute intensity calibration of the all-sky cameras were made, a lower limit of the intensity of the N_2^+ 427.8 nm blue emission can be estimated.

In Figure 7, we reproduced one of the raw camera frames taken by the South Pole camera during our first case study (12 August 2007). Figure 7 top left image is 427.8 nm and the bottom right is 630 nm. The night sky starlight background in the 427.8 nm wavelength region is about 2 *R* per angstrom, and the filter passband was 20 angstroms, giving a minimum background illumination of 40 *R* in the 427.8 nm image. In the blue image near zenith, between the poleward bright cusp aurora and the equatorward dimmer plasma sheet precipitation, there is a region with very little auroral luminosity. It can be assumed that this would be at least 40 *R* background constituting a lower limit. Using this number, we can provide calibration of the plot of Figure 7 (right). We show a calibrated intensity scale in Rayleighs, signifying that the aurora is at least as bright as the scale shows. Accordingly, in the cusp aurora, the intensity of the highly structured bright rays can reach 400 *R* or more. Comparing this to the unaccelerated magnetosheath electrons shows that the electrons must undergo significant acceleration and gain about a factor of 3 in energy before impacting the atmosphere.

These brightest auroral features in the cusp 427.8 nm emission are highly dynamic and vary from frame to frame and show relatively small-scale structured features (at 15:57:31, 16:22:07, and 16:14:02 as seen from Figure 3). This type of structuring is consistent with Alfvén wave-accelerated electrons, since similar structuring is seen in the initial breakup auroras on the nightside, which are also produced by wave-accelerated

electrons. The importance of wave-accelerated electrons was emphasized in the nightside aurora [*Mende et al.*, 2003]. Results from the FAST satellite showed that the dayside aurora and cusp precipitation have the characteristic Alfvén wave-accelerated electrons [*Chaston et al.*, 2007]. *Newell et al.* [2009] reviewed the frequency of occurrence of broadband or Alfvénic aurora caused by wave-accelerated electrons using DMSP satellite measurements. The waves are most likely produced at the dayside reconnection sites at the magnetopause, and these waves propagate down to the ionosphere picking up magnetosheath electrons and ions and accelerating them.

Although this work contained only two case studies, both involved several THEMIS satellites which produced consistent results.

5. Conclusions

From two case studies, we have clear evidence that the midday soft cusp aurora exhibiting high ratios of 630 to 427.8 nm emission appears in the region of open field lines [*Khan et al.*, 2003] and that the magnetosheath is the source of the cusp auroral particles. The THEMIS magnetic field and the plasma density data pinpointed the location of the magnetopause, which was mapped to the ionosphere using the Tsyganenko-96 field model. These coordinated observations proved that the conventional dayside cusp aurora is on open field lines and it is therefore direct precipitation from the magnetosheath. The cusp aurora also contained significant highly structured N_2^+ 427.8 nm emission. The THEMIS measurements of the magnetosheath particle energy and density were compared to the intensity of the structured N_2^+ 427.8 nm emissions in the cusp aurora. The comparison showed that the precipitating magnetosheath particles had to be accelerated. The energy range and the highly structured nature of the 427.8 nm aurora suggest Alfvénic auroras produced by an electron acceleration mechanism driven by dispersive Alfvén waves. There is evidence from FAST satellite data that the dayside cusp aurora is frequently of the Alfvénic type [*Chaston et al.*, 2007].

The field modeling used in mapping the dayside aurora to the magnetopause boundary is sufficiently accurate to support our conclusions. In the subsolar region of the magnetosphere the magnetic field is relatively strong and is not subject to large deviations from the models. Therefore, we are certain that our conclusion regarding the magnetosheath source of the conventional cusp auroras is valid and it is not a mapping error.

The other distinct auroral feature on the dayside is the 427.8 nm aurora located equatorward of the mapped magnetopause boundary and consequently located inside the magnetosphere. Although this aurora is usually a weak precipitating flux, it is created by hard plasma sheet electrons that have drifted in from the nightside.

Acknowledgments
This study was funded by NSF under grant 1141961 entitled "Auroral Signatures of Solar wind Magnetospheric Coupling" at the University of California, Berkeley. Parts of this work were also supported by the NASA THEMIS program under contract NAS5-02099. The authors also wish to express their gratitude to the engineering and field teams who made the U.S. Automatic Geophysical Observatory imaging observations possible. The authors wish to acknowledge K.H. Glassmeier, U. Auster, and W. Baumjohann for the use of FGM data provided under the lead of the Technical University of Braunschweig and with financial support through the German Ministry for Economy and Technology and the German Center for Aviation and Space (DLR) under contract 50 OC 0302. The ground-based optical data for South Pole and the U.S. Automatic Geophysical Observatories can be accessed at http://sprg.ssl.berkeley.edu/atmos/ago_data.html. The results of field line mapping for the THEMIS satellite footprints are attached as supporting information.

References

Angelopoulos, V., et al. (2008), First results from the THEMIS mission, *Space Sci. Rev.*, doi:10.1007/s11214-008-9378-4.

Auster, H. U., et al. (2008), The THEMIS Fluxgate Magnetometer, *Space Sci. Rev.*, doi:10.1007/s11214-008-9365-9.

Chaston, C. C., C. W. Carlson, J. P. McFadden, R. E. Ergun, and R. J. Strangeway (2007), How important are dispersive Alfvén waves for auroral particle acceleration?, *Geophys. Res. Lett.*, *34*, L07101, doi:10.1029/2006GL029144.

Chisham, G., M. P. Freeman, T. Sotirelis, R. A. Greenwald, M. Lester, and J. Villain (2005), A statistical comparison of SuperDARN spectral width boundaries and DMSP particle precipitation boundaries in the morning sector ionosphere, *Ann. Geophys.*, *23*, 733–743, doi:10.5194/angeo-23-733-2005.

Eather, R. H., and S. B. Mende (1971), Airborne observation of auroral precipitation patterns, *J. Geophys. Res.*, *76*, 1740–1755, doi:10.1029/JA076i007p01746.

Eather, R. H., S. B. Mende, and E. J. Weber (1979), Dayside aurora and relevance to substorm current systems and dayside merging, *J. Geophys. Res.*, *84*, 3339–3359, doi:10.1029/JA084iA07p03339.

Fuselier, S. A., Frey, H. U., Trattner, K. J., Mende, S. B., Burch, J. L. (2002), Cusp aurora dependence on interplanetary magnetic field B_z, *J. Geophys. Res.*, *107*(A7), 1111, doi:10.1029/2001JA900165.

Gattinger, R. L., A. Vallance Jones, J. H. Hecht, D. J. Strickland, and J. Kelly (1991), Comparison of ground-based optical observations of N_2 second positive to N^- first negative emission ratios with electron precipitation energies inferred from the Sondre Stromfjord radar, *J. Geophys. Res.*, *96*, 11,341–11,351, doi:10.1029/91JA01015.

Heikkila, W. J., and J. D. Winningham (1971), Penetration of magnetosheath plasma to low altitudes through the dayside magnetospheric cusps, *J. Geophys. Res.*, *76*, 883–891, doi:10.1029/JA076i004p00883.

Hubert, B., S. E. Milan, A. Grocott, C. Blockx, S. W. H. Cowley, and J.-C. GéRard (2006), Dayside and nightside reconnection rates inferred from IMAGE FUV and Super Dual Auroral Radar Network data, *J. Geophys. Res.*, *111*, A03217, doi:10.1029/2005JA011140.

Johnsen, M. G., D. A. Lorentzen, J. M. Holmes, and U. P. Løvhaug (2012), A model based method for obtaining the open/closed field line boundary from the cusp auroral 6300 Å [OI] red line, *J. Geophys. Res.*, *117*, A03319, doi:10.1029/2011JA016980.

Khan, H., M. Lester, J. A. Davies, S. E. Milan, and P. E. Sandholt (2003), Multi-instrument study of the dynamic cusp during dominant IMF B_y conditions, *Ann. Geophys.*, *21*, 693, doi:10.5194/angeo-21-693-2003.

Lockwood, M., H. C. Carlson Jr., and P. E. Sandholt (1993), Implications of the altitude of transient 630-nm dayside auroral emissions, *J. Geophys. Res.*, *98*, 15,571–15,587, doi:10.1029/93JA00811.

Lockwood, M., J. A. Davies, J. Moen, A. P. van Eyken, K. Oksavik, I. W. McCrea, and M. Lester (2005), Motion of the dayside polar cap boundary during substorm cycles: II. Generation of poleward-moving events and polar cap patches by pulses in the magnetopause reconnection rate, *Ann. Geophys.*, *23*, 3513–3532, doi:10.5194/angeo-23-3513-2005.

Longden, N., G. Chisham, M. P. Freeman, G. A. Abel, and T. Sotirelis (2010), Estimating the location of the open-closed magnetic field line boundary from auroral images, *Ann. Geophys.*, *28*, 1659–1678, doi:10.5194/angeo-28-1659-2010.

Mende, S. B. Carlson, C. W. Frey, H. U. Peticolas, L. M. Østgaard, N. (2003), FAST and IMAGE-FUV observations of a substorm onset, *J. Geophys. Res.*, *108*(A9), 1344, doi:10.1029/2002JA009787.

Mende, S. B., et al. (2009), Observations of Earth space by self-powered stations in Antarctica, *Rev. Sci. Instrum.*, *80* 124501-124501-19, doi:10.1063/1.3262506.

Milan, S. E., G. Provan, and B. Hubert (2007), Magnetic flux transport in the Dungey cycle: A survey of dayside and nightside reconnection rates, *J. Geophys. Res.*, *112*, A01209, doi:10.1029/2006JA011642.

Newell, P. T., T. Sotirelis, K. Liou, C. Meng, and F. J. Rich (2006), Cusp latitude and the optimal solar wind coupling function, *J. Geophys. Res.*, *111*, A09207, doi:10.1029/2006JA011731.

Newell, P. T., T. Sotirelis, and S. Wing (2009), Diffuse, monoenergetic, and broadband aurora: The global precipitation budget, *J. Geophys. Res.*, *114*, A09207, doi:10.1029/2009JA014326.

Rees, M. H., and D. Luckey (1974), Auroral electron energy derived from ratio of spectroscopic emissions. I—Model computations, *J. Geophys. Res.*, *79*, 5181–5186, doi:10.1029/JA079i034p05181.

Rosenberg, T. J. (2000), Recent results from correlative ionosphere and magnetosphere studies incorporating Antarctic observations, *Adv. Space Res.*, *25*(7-8), 1357–1366, doi:10.1016/S0273-1177(99)00645-6.

Sandholt, P. E., H. C. Carlson, and A. Egeland (Eds.) (2002), *Dayside and Polar Cap Aurora*, Kluwer Acad., Dordrecht, Netherlands.

Shepherd, G. G., J. F. Pieau, F. Creutzberg, A. G. McNamara, J. C. Gerard, D. J. McEwen, B. Delana, and J. H. Whitteker (1976), Rocket and ground-based measurements of the dayside magnetospheric cleft from Cape Parry, N. W. T, *Geophys. Res. Lett.*, *3*, 69–72, doi:10.1029/GL003i002p00069.

Strickland, D. J., R. R. Meier, J. H. Hecht, and A. B. Christensen (1989), Deducing composition and incident electron spectra from ground-based auroral optical measurements: Theory and model results, *J. Geophys. Res.*, *94*, 13,527–13,539, doi:10.1029/JA094iA10p13527.

Tsyganenko, N. (1995), Modeling the Earth's magnetospheric magnetic field confined within a realistic magnetopause, *J. Geophys. Res.*, *100*(A4), 5599–5612, doi:10.1029/94JA03193.

Winningham, J. D., and W. J. Heikkila (1974), Polar cap auroral electron fluxes observed with ISIS 1, *J. Geophys. Res.*, *79*, 949–957, doi:10.1029/JA079i007p00949.